

# Systematical calculations of the $^{136}\text{Xe}(^{136}\text{Xe},xn)^{272-x}\text{Hs}$ reaction: Effects of quasifission in the early stage of the fusion process

Zu-Hua Liu<sup>1</sup> and Jing-Dong Bao<sup>2,3</sup>

<sup>1</sup>China Institute of Atomic Energy, Beijing 102413, People's Republic of China

<sup>2</sup>Department of Physics, Beijing Normal University, Beijing 100875, People's Republic of China

<sup>3</sup>Center of Theoretical Nuclear Physics, National Laboratory of Heavy Ion Accelerator, Lanzhou 730000, People's Republic of China

(Received 3 March 2010; published 16 April 2010)

We have reevaluated the  $^{136}\text{Xe}(^{136}\text{Xe},xn)^{272-x}\text{Hs}$  reaction with a modified fusion-by-diffusion model. In this model, the early dynamics of neck growth is taken into account in terms of the two-dimensional Langevin equation. By numerically solving the dynamic equations, the probability distribution of the separation between the surfaces of two approaching nuclei at the injection point in an asymmetric fission valley is obtained. Before reaching the asymmetric fission valley, the strong electrostatic repulsion may force the system to re-integrate in a quasifissionlike process. We find that more than 80% of quasifission events occur during the transition from dinuclear to mononuclear regimes for the  $^{136}\text{Xe} + ^{136}\text{Xe}$  reaction. This observation gives credence to the conjecture that the quasifission reaction channel most likely occurs in an early stage of collective motion. By incorporating this essential physical ingredient into the calculations, the modified fusion-by-diffusion model nicely accounts for the experiment of the  $^{136}\text{Xe} + ^{136}\text{Xe}$  reaction performed in Dubna.

DOI: [10.1103/PhysRevC.81.044606](https://doi.org/10.1103/PhysRevC.81.044606)

PACS number(s): 24.10.-i, 24.60.-k, 25.70.Jj

## I. INTRODUCTION

Under the present experimental conditions, the hot fusion reactions of  $^{48}\text{Ca}$  with actinide targets have proven to be the most effective way to produce more neutron-rich superheavy nuclei with heavier masses. In terms of such hot fusion reactions, remarkable progress has been made in the synthesis of superheavy elements within the past few years. Elements with  $Z = 112$ – $116$  were produced in the reactions of  $^{238}\text{U}$ ,  $^{242,244}\text{Pu}$ ,  $^{243}\text{Am}$ , and  $^{245,248}\text{Cm}$  targets with  $^{48}\text{Ca}$  beams [1–4]. Recently, element 118 was produced in Dubna in the  $3n$  evaporation channel of the  $^{48}\text{Ca} + ^{249}\text{Cf}$  complete fusion reaction [5]. However, the reactions of  $^{48}\text{Ca}$  with actinide targets have their own limitations. They cannot advance further than element 118 since the californium nucleus is the heaviest actinide that can be used as a target material for this purpose. Moreover, the neutron-rich nuclides synthesized most frequently,  $^{294}118$  ( $N = 176$ ) and  $^{293}116$  ( $N = 177$ ), are still seven or eight neutrons away from the predicted neutron magic number,  $N = 184$ .

Other ways to produce neutron-rich isotopes of superheavy nuclei were comprehensively searched for [6]. One possibility is to use neutron-rich radioactive nuclei as beams. Although not presently in practice, neutron-rich radioactive nuclei heavier than  $^{48}\text{Ca}$  must be used in future experiments to synthesize superheavy nuclei in the central region of the predicted “island of stability.” One of the problems with using heavy radioactive nuclei is the hindrance to the formation of a compound nucleus. Usually the dynamic hindrance to fusion for the more-or-less mass-symmetric reaction systems, as compared to the mass-asymmetric reaction systems of  $^{48}\text{Ca}$  with actinide, would dramatically increase [7]. Unfortunately, the fusion hindrance factor or the fusion probability is very uncertain in the present theoretical predictions. Therefore, it is quite necessary to estimate this factor using test reactions with known nuclei. One of the symmetric reactions,  $^{136}\text{Xe}(^{136}\text{Xe},xn)^{272-x}\text{Hs}$ , seems to be suitable for this purpose.

An experiment on the synthesis of hassium in the  $^{136}\text{Xe} + ^{136}\text{Xe}$  fusion reaction was performed recently in Dubna, and not one event was detected at the level of about 4 pb [8]. Because the experimental values of the fusion hindrance factor for such reactions are still unknown, an attempt to synthesize a superheavy element in the fusion of two heavy nuclei, more or less equal in mass, should be continued. Therefore, more realistic estimations of the formation cross section for such reactions are greatly needed.

Siwek-Wilczyńska *et al.* [9] have analyzed the  $^{136}\text{Xe} + ^{136}\text{Xe}$  fusion reaction with the fusion-by-diffusion model [10,11]. The evaporation residue (ER) cross section for production of the  $^{270}\text{Hs}$  isotope in the  $2n$  channel calculated by this model is of an order of 10 pb, which exceeds the experimental data by orders of magnitude [8,9].

The fusion-by-diffusion model brings out the basic physics of the observed hindrance with an elementary formula. Similar models have been developed by Zagrebaev and Greiner [6] and Aritomo [12]. However, it is worth noting that in formulating the model, numerous approximations were introduced. One of these is that the dynamics of the neck growth phase was bypassed by introducing an adjustable parameter  $s$ , which is the separation between the surfaces of the approaching nuclei at which injection into the asymmetric fission valley takes place. In the calculation of Siwek-Wilczyńska *et al.* [9],  $s = 0$  was assumed. This may bring about uncertainty in the fusion hindrance factor because it sensitively depends on the parameter  $s$  for the reaction systems with a large Coulomb parameter,  $z = Z_1 Z_2 / (A_1^{1/3} + A_2^{1/3})$ . In addition, the possibility of quasifission competition during the evolution process from dinuclear to mononuclear regimes is also bypassed using this approach. As will be seen, quasifission strongly competes with complete fusion in this stage for heavy, more-or-less symmetric reaction systems, such as  $^{136}\text{Xe} + ^{136}\text{Xe}$ . In the present work, dynamic evolution from a dinucleus to a mononucleus is taken into account. As a result,  $s$  is no

longer an adjustable parameter. In addition, the competition between fusion and quasifission in this transition stage is included in the model. These improvements should increase the reliability of the theoretical predictions upon the hindrance to fusion.

The cross section of a superheavy nucleus produced in a heavy-ion fusion-evaporation reaction is calculated as follows:

$$\sigma_{\text{ER}}(E) = \pi \tilde{\chi}^2 \sum_{l=0}^{\infty} (2l+1) P_{\text{capt}}(E, l) P_{\text{CN}}(E, l) P_{xn}(E, l). \quad (1)$$

Here  $P_{\text{capt}}$  is the capture probability of the colliding nuclei after overcoming the Coulomb barrier and moving up to the contact point.  $P_{\text{CN}}$  defines the probability that the system will go from the configuration of two nuclei in contact into the configuration of the compound nucleus (CN). Finally,  $P_{xn}$  represents the survival probability of the excited compound nucleus after evaporation of  $x$  neutrons in the cooling process. We calculate the last factor  $P_{xn}$  using a more-or-less convenient method (for details see Ref. [13]). Only the smooth part of the fission barrier (i.e., the deformation energy of macroscopic liquid-drop model,  $B_{\text{LD}}$ ) has to be specified here. The value of  $B_{\text{LD}}$  for the nuclei under consideration should be about 0.5 MeV, as estimated from the liquid-drop approximation [14], if the shape of the relevant nuclei in the ground state is spherical. However, nuclei situated in close proximity to the  $N = 162$  shell have a large deformation ( $\beta \approx 0.24$ ) in the ground state, which is very close to the nuclear deformation at the top position of the liquid-drop fission barrier. Therefore,  $B_{\text{LD}}$  would be zero or even slightly negative in value compared to the fission barrier position. We set  $B_{\text{LD}} = 0$  [15] in this work. In what follows, Secs. II–IV describe the dynamic processes of capture and fusion; the first two factors in Eq. (1) are specified there. The results and discussion are presented in Sec. V. Finally, a brief summary is given in Sec. VI.

## II. CAPTURE

We use the surface friction model (SFM) [16–18] to calculate the capture probability  $P_{\text{capt}}$ . In this model, the capture process is described by the dissipation-fluctuation dynamics (i.e., the Langevin equation),

$$\frac{d}{dt} p_R = - \left( \frac{\partial V}{\partial R} - \frac{L^2}{\mu R^3} \right) - K_R \frac{p_R}{\mu} + L_R(t), \quad (2)$$

where  $\mu$  denotes the reduced mass in the entrance channel and  $L = \hbar l$  is the incident orbital angular momentum of the system. The conservative potential  $V(R)$  consists of nuclear and Coulomb parts. In the present work, the nuclear potential  $V_n$  is evaluated with a folding procedure [17]. The nuclear density in the folding is calculated in terms of the Hartree-Fock approximation so that the shell effect on the capture process is properly taken into account. The radial friction form factor has the following form:

$$K_R = K_R^0 \left( \frac{\partial V_n(R)}{\partial R} \right)^2 \quad (3)$$

with the strength parameter  $K_R^0 = 4 \times 10^{-23} \text{ s MeV}^{-1}$  [19].

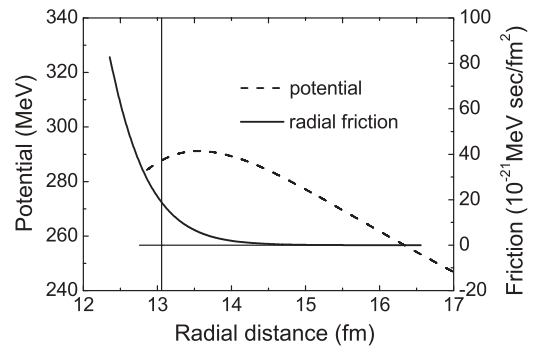


FIG. 1. The radial potential and the radial form factor of the friction for the  $^{136}\text{Xe} + ^{136}\text{Xe}$  system, calculated with SFM. The vertical line indicates the top position of the barrier.

In Fig. 1, the potential and the radial friction form factor for the  $^{136}\text{Xe} + ^{136}\text{Xe}$  system are shown as a function of the relative distance. It is worth noting from the figure that friction between the two colliding nuclei already exists beyond the barrier top for heavy systems such as  $^{136}\text{Xe} + ^{136}\text{Xe}$ .

The Langevin force  $L_R(t)$  in Eq. (2) is a Gaussian white noise with zero mean and  $\delta$  correlation, that is,

$$\langle L_R(t) \rangle = 0, \quad \langle L_R(t) L_R(t') \rangle = 2D_R \delta(t - t'). \quad (4)$$

The radial diffusion coefficient is determined by assuming that the fluctuation-dissipation theorem is valid,  $D_R = K_R T$ , where the temperature  $T$  is calculated from the internal excitation energy  $E^*$  along each trajectory,  $T = \sqrt{E^*/a}$ , and the value  $a = A/8 \text{ MeV}^{-1}$  is used for the level density parameter.

The dissipation of angular momentum is not taken into account in the SFM calculations for the following reasons. First, only low angular momentum components are involved in the synthesis of superheavy elements. Second, the tangential friction is small beyond the barrier top for not-too-high angular momentum components. Hence the effect of angular momentum dissipation on the capture probability is negligible. Figure 2 shows the excitation function of the capture probability for the system  $^{136}\text{Xe} + ^{136}\text{Xe}$  with incident orbital angular momentum  $l = 0$ . The results clearly demonstrate that the extra-push energy is needed in the capture process for the heavy reaction systems.

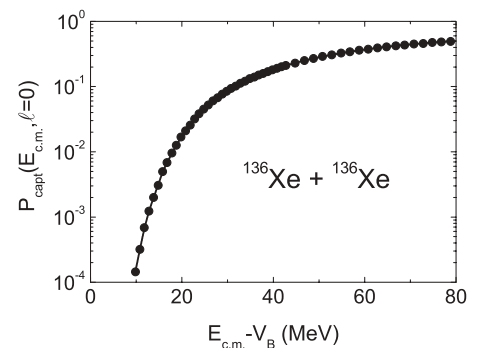


FIG. 2. Energy dependence of the capture probability obtained by SFM for the system  $^{136}\text{Xe} + ^{136}\text{Xe}$  with incident orbital angular momentum  $l = 0$ .

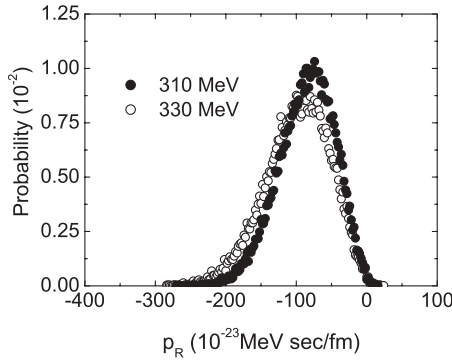


FIG. 3. Calculated radial momentum distributions at the contact point for the system  $^{136}\text{Xe} + ^{136}\text{Xe}$  at the incident energies of 310 and 330 MeV, respectively.

In Fig. 3, the radial momentum  $p_R$  distributions of the  $^{136}\text{Xe} + ^{136}\text{Xe}$  system at the contact point are presented at two incident energies.

### III. EVOLUTION FROM A DINUCLEUS TO A MONONUCLEUS REGIME

After contact, a rapid initial growth of the neck brings the reaction system from a dinuclear regime to a mononuclear regime. In the following, we apply the liquid-drop model of nuclear collisions [20,21] to describe this dynamic process. In the model, the geometrical shape of the system is parametrized in terms of two spheres that represent the approaching nuclei and are joined by a conical or cylindrical neck. The configuration is described through three dimensionless quantities:  $\varrho = R/(R_1 + R_2)$ ,  $\nu = \sin\theta/\sin\theta_{\max}$ , and  $D = [(R_1 - R_2)/(R_1 + R_2)]^2$ , where  $\theta$  is the semiopening angle and  $\sin\theta_{\max} = (R_1 - R_2)/R$  [20]. For a symmetric system, the neck is cylindrical in shape, and correspondingly,  $\nu$  is defined as the half-width of the neck divided by  $R_1$ . The dimensionless variables  $\varrho$ ,  $\nu$ , and  $D$  measure, respectively, the distance between the two nuclear centers, the neck size, and the mass asymmetry of the system. In the present work, only the variables  $\varrho$  and  $\nu$  are concerned. Following Aguiar *et al.* [21], we use the related dimensionless variables

$$S = \frac{\varrho^2 - 1}{K_1}, \quad N = \frac{\nu}{K_2}, \quad (5)$$

where  $K_1 = 2R_0/(R_1 + R_2)$  and  $K_2 = R_0/(2\bar{R})$ .  $R_0$  stands for the radius of the compound nucleus and  $\bar{R} = R_1 R_2 / (R_1 + R_2)$  is the reduced radius of the system. Note that the lowercase  $s$  and capital  $S$  have the same meaning but are different in units. They both measure the distance between the surfaces of approaching nuclei, however, and are in units of femtometers and  $R_0$  for the variables  $s$  and  $S$ , respectively.

The kinetic energy  $E_k$  of the system with two degrees of freedom  $S$  and  $N$  is expressed as

$$E_k = \frac{1}{2} M_{SS} \dot{S}^2 + \frac{1}{2} M_{NN} \dot{N}^2, \quad (6)$$

where  $M_{SS} = MR_0^2/(K_1 K_2)^3$  and  $M = M_1 + M_2$  is the total mass of the system. Recently, Zhao *et al.* [22] have calculated the mass parameter of neck motion,  $M_{\Delta\Delta}$ , for the symmetric systems  $^{90}\text{Zr} + ^{90}\text{Zr}$ ,  $^{110}\text{Pd} + ^{110}\text{Pd}$ , and  $^{138}\text{Ba} + ^{138}\text{Ba}$  by

means of a microscopic transport model. Here  $\Delta$  defines the total width of the neck. According to the relation between  $\Delta$  and  $N$ , we have  $M_{NN} = M_{\Delta\Delta} \bar{R}^2 K_2^2$  with the values of  $M_{\Delta\Delta}$  taken from the data of the  $^{138}\text{Ba} + ^{138}\text{Ba}$  system [22]. This should be reasonable because the reaction systems  $^{136}\text{Xe} + ^{136}\text{Xe}$  and  $^{138}\text{Ba} + ^{138}\text{Ba}$  are very similar. The potential  $V$  and friction coefficients  $\Gamma_S$ ,  $\Gamma_N$  depend on the coordinates  $S$ ,  $N$ , and  $D$ . They are given in Ref. [21]. With the kinetic and potential energies, we can construct the Lagrangian  $\mathcal{L} = E_k - V$ . The equations of motion are obtained from the Lagrangian and Rayleigh dissipation functions and are explicitly written as

$$\frac{d}{dt} P_S = -\frac{\partial V}{\partial S} - \Gamma_S \frac{P_S}{M_{SS}} + L_S(t), \quad (7)$$

$$\frac{d}{dt} P_N = \frac{1}{2} \frac{\partial M_{NN}}{\partial N} \left( \frac{P_N^2}{M_{NN}^2} \right) - \frac{\partial V}{\partial N} - \Gamma_N \frac{P_N}{M_{NN}} + L_N(t), \quad (8)$$

where  $\langle L_q(t) \rangle = 0$  and  $\langle L_q(t) L_{q'}(t') \rangle = 2D_{qq'} \delta(t - t')$ ,  $q, q' = N, S$ .

In Eqs. (7) and (8),  $P_S = M_{SS} \dot{S}$  and  $P_N = M_{NN} \dot{N}$  stand for the momenta in the degrees of freedom  $S$  and  $N$ . In Ref. [21], the kinetic energy of the neck motion was neglected, which results in the left-hand side of Eq. (8) being zero. The result of Zhao *et al.* [22] showed that around the contact configuration the kinetic energy of the neck motion is not negligible when compared to that of radial motion. Introducing the kinetic energy of neck motion in the Lagrangian brings about the  $dP_N/dt$  term in the left-hand side of Eq. (8). Besides, because the mass parameter  $M_{\Delta\Delta}$  is a function of the neck width, the dynamic equation (8) also includes a term relevant to the derivative of  $M_{NN}$ . We find that these modifications are necessary and appropriate for the reasonable solution of equations. In principle, the mass parameter  $M_{NN}$  should also depend on the degree of freedom  $S$ . However, as shown in the following, in the process of neck formation only a very limited radial range close to  $S = 0$  is involved, and in this region the coupling between the radial and neck motions is relatively weak. Therefore, to simplify the calculation we assume that  $\partial M_{NN}/\partial S = 0$ . The diffusion coefficient tensor  $D_{qq'}$  is related to the friction coefficient  $\Gamma_q$  by the dissipation-fluctuation theorem,

$$D_{qq'} = T \Gamma_q \delta_{qq'}(q, q' = S, N). \quad (9)$$

The connection between the two processes just described is a subtle problem that must be addressed. Naturally, the two processes are in succession, so the result of the first step may give the initial condition of the second step. According to this approach [19], we set the initial momentum value of radial motion,

$$P_S(0) = \sqrt{\frac{M_{SS}}{\mu}} p_R. \quad (10)$$

As the two nuclei approach the contact point, the diffusive surfaces of the two nuclei overlap. The nucleons in the overlap most probably fill in the neck region because of the incompressibility of nuclear matter. For heavy reaction systems, for instance  $^{118}\text{Pd} + ^{118}\text{Pd}$ , there are more than 16 nucleons

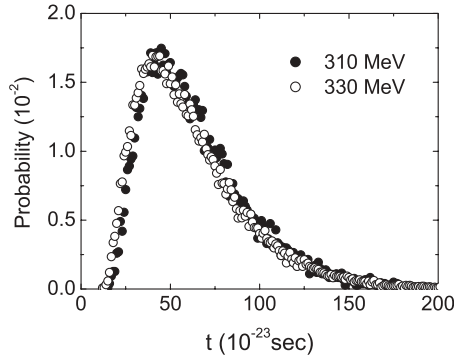


FIG. 4. Probability distributions of transition times for the system  $^{136}\text{Xe} + ^{136}\text{Xe}$  at the incident energies of 310 and 330 MeV.

in the neck [23]. As a consequence, the dinuclear system already has developed a neck at the contact configuration. Moretto *et al.* [24] assumed the neck size to be proportional to the reduced radius  $\bar{R}$ . The recent calculation based on a microscopic transport model [22] has shown that the neck size of the  $^{138}\text{Ba} + ^{138}\text{Ba}$  reaction system at the contact configuration is close to the value of this estimation. As the neck formed, the potential energy decreases by the amount of  $\Delta V$ . We assume that this part of the potential energy transforms into the kinetic energy of neck motion. Based on these assumptions, we approximately set the initial values of neck motion as

$$N(0) = \frac{\bar{R}}{2R_0}, \quad P_N(0) = \sqrt{2M_{NN}\Delta V}. \quad (11)$$

For the  $^{136}\text{Xe} + ^{136}\text{Xe}$  reaction, we find  $N(0) \simeq 0.2$  and  $\Delta V = 10$  MeV.

Swiaticki [20] has taken  $v^2 = \frac{1}{2}$  to be the boundary between the dinuclear and mononuclear regimes. Figure 4 shows the transition time distributions for the system  $^{136}\text{Xe} + ^{136}\text{Xe}$  at two incident energies. Here the transition time is defined as the time when the reaction system arriving at the mononuclear regime (i.e., injection into the asymmetric fission valley) takes place. The figure shows that the transition takes place in a very short time, about the order of  $10^{-22}$  s.

In Fig. 5, we plot the probability distribution of  $s$ ,  $f(s)$ , where  $s$  is the separation between the surfaces of two interaction nuclei at the injection point. It is worth noting that

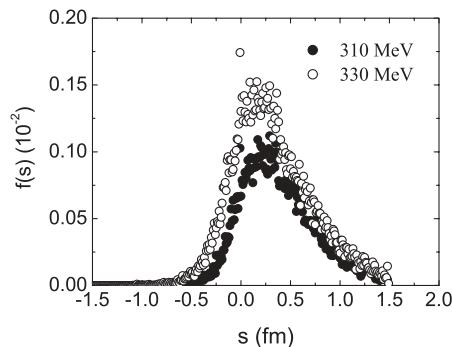


FIG. 5. The probability distributions of  $s$  for the system  $^{136}\text{Xe} + ^{136}\text{Xe}$  at the incident energies of 310 and 330 MeV.

the distribution is not normalized because of the quasifission effect; for higher energy the system has a larger probability of injecting into the asymmetric fission valley. This is because during the dynamic evolution from dinuclear to mononuclear regimes the strong electrostatic repulsion may force the system to re-integrate in a quasifissionlike process instead of forming a mononucleus. If we refer to the configuration space between the dinuclear and mononuclear regimes as a doorway to fusion, then the quasifission competition greatly reduces the fusion probability for the system under consideration to go through this doorway state.

#### IV. DIFFUSION IN THE ASYMMETRIC FISSION VALLEY

For heavy systems, the saddle-point shape shrinks below the length of the contact configuration. After contact a rapid growth of the neck brings the system to the injection point in the asymmetric fission valley located outside the saddle-point barrier. Hence automatic fusion will no longer take place. Starting from the injection point, the system diffuses uphill, and with some probability it reaches the compound nucleus configuration owing to the thermal fluctuation. The equation describing this process is the Smoluchowski partial differential equation in the fusion-by-diffusion model [10,11,13,25–27]. It is assumed in the model that the probability of overcoming the barrier is given by [10,11]

$$P_{\text{CN}} = \frac{1}{2} \text{erfc}[\sqrt{B(s)/T}], \quad (12)$$

where  $B(s)$  is the barrier height of the opposing fusion along the asymmetric fission valley on the way from the injection point to the saddle, and  $T$  is the effective temperature.

In our approach, the thermal fluctuation in the capture and neck growth processes results in a distribution of  $s$ , the separation between two interacting nuclei at the injection point. This causes the barrier height  $B(s)$  to have a distribution. Therefore, the fusion probability should be given by a convolution of Eq. (12) over the distribution  $f(s)$ :

$$P_{\text{CN}} = \frac{1}{2} \int_{-\infty}^{\infty} \text{erfc}[\sqrt{B(s)/T}] f(s) ds. \quad (13)$$

In Fig. 6 we show the fusion probability (fusion hindrance) for the  $^{136}\text{Xe} + ^{136}\text{Xe}$  system as a function of the excitation energy of compound nucleus. The dashed line is calculated with Eq. (12) and assumes the injection point is at the separation distance  $s = 0$ , while the solid line is calculated using Eq. (13) with the distribution of  $s$  predicted by the dynamic equations of neck motion. It is indeed seen from the figure that after the dynamic evolution of the neck is taken into account, the fusion probability decreases by one order of magnitude.

#### V. RESULTS AND DISCUSSION

In Fig. 7, we plot the ER cross sections for  $1n$ ,  $2n$ , and  $3n$  evaporation channels in the  $^{136}\text{Xe} + ^{136}\text{Xe}$  reaction, which leads to the formation of  $^{271}\text{Hs}$ ,  $^{270}\text{Hs}$ , and  $^{269}\text{Hs}$  isotopes. The dash-dotted, dashed, and solid lines in the figure are the

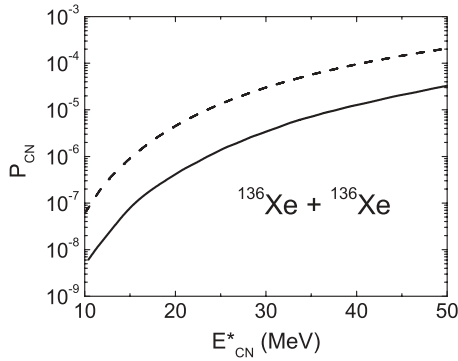


FIG. 6. Fusion probability as a function of the excitation energy of a compound nucleus for the  $^{136}\text{Xe} + ^{136}\text{Xe}$  system. The dashed line is calculated with Eq. (12) assuming  $s = 0$ ; the solid line is calculated with Eq. (13).

predictions of Zagrebaev and Greiner [6], Siwek-Wilczyńska *et al.* [9], and the present work, respectively. Our calculated maximum ER cross sections in  $1n$  and  $2n$  channels are 0.45 and 0.55 pb, respectively, orders of magnitude lower than those of Siwek-Wilczyńska *et al.* [9].

In order to look for the origins of this difference, as an example we present in Fig. 8 the ER cross sections for the  $2n$  channel in the  $^{136}\text{Xe} + ^{136}\text{Xe}$  reaction by using three different approaches for the fusion probability  $P_{\text{CN}}$ . The capture probability is calculated in terms of the surface friction model [16–18] for all these three cases. The dashed line represents the prediction with  $P_{\text{CN}}$  calculated by Eq. (12) and assumes  $s = 0$ . The dash-dotted line illustrates the result in which  $P_{\text{CN}}$  is evaluated with Eq. (13) but neglects the quasifission competition during the dynamic evolution process of neck growth. This is realized by normalizing the distribution  $f(s)$ . By comparing these two lines, one can examine the effect of the  $s$  distribution on the formation cross section. As shown, the neck grows in a short time scale. Hence, at least at first, the neck growth can be considered as proceeding with the overall elongation and asymmetry of the system approximately frozen [11]. The small difference between the ER excitation

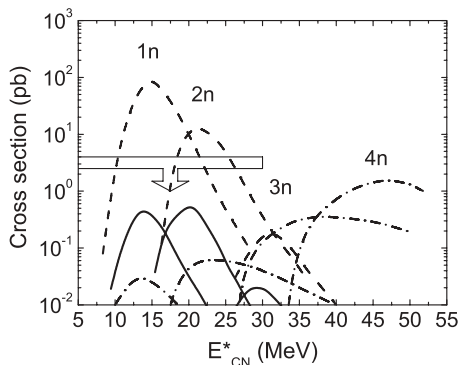


FIG. 7. Predicted evaporation residue cross sections for  $1n$ ,  $2n$ , and  $3n$  evaporation channels in the  $^{136}\text{Xe} + ^{136}\text{Xe}$  reaction, which leads to the formation of  $^{271}\text{Hs}$ ,  $^{270}\text{Hs}$ , and  $^{269}\text{Hs}$  isotopes. The dash-dotted, dashed, and solid lines are the results of Ref. [6], Ref. [9], and the present work, respectively. The hollow bar shows the upper limit of the experimental ER cross sections in this reaction [8].

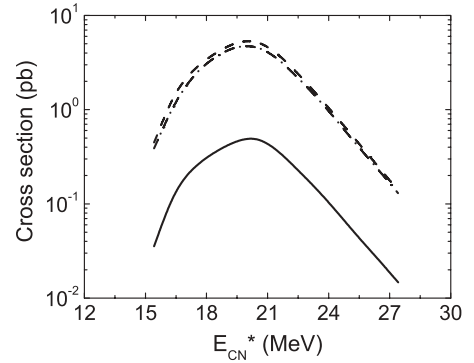


FIG. 8. A comparison of the ER cross sections in the  $2n$  channel of the  $^{136}\text{Xe} + ^{136}\text{Xe}$  reaction evaluated with three different approaches of fusion probability  $P_{\text{CN}}$ . The dashed line represents the prediction with  $P_{\text{CN}}$  calculated by Eq. (12) and assumes  $s = 0$ . The dash-dotted line illustrates the result in which  $P_{\text{CN}}$  is evaluated with Eq. (13) and neglects quasifission competition. The solid line displays the prediction of the present approach.

functions with these two approaches means that the frozen assumption [11] is satisfied. The solid line in the figure shows the prediction of the present approach. At this point one can conclude that the main reason for the reduction of the ER cross section is the quasifission competition during the dynamic process of neck formation.

Figure 9 displays the quasifission probability as a function of the excitation energy of a compound nucleus in the transition period. It is clearly shown that before injection into the asymmetric fission valley the system disintegrates with more than 80% probability into the quasifission channel owing to the strong electrostatic repulsion. This observation substantiates Oganessian’s conjecture [15] that the quasifission reaction channel most likely occurs at the earliest stage of collective motion.

There is always room for improvement when studying the early dynamics of neck growth. The preceding description of the geometrical shape of the system has a clear advantage because it allows a simple polynomial approximation for the liquid-drop potential energy and the analytic formula for the one-body dissipation function. However, a conical or cylindrical neck may not be so realistic in shape. In this connection, the potential energy and dissipation function evaluated with

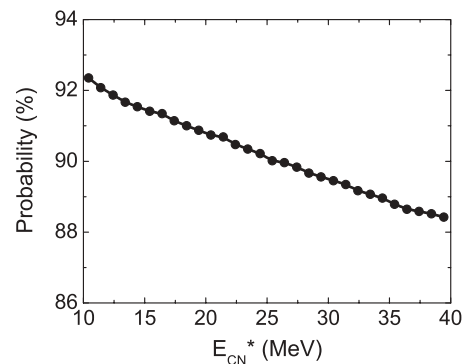


FIG. 9. The quasifission probability of the  $^{136}\text{Xe} + ^{136}\text{Xe}$  reaction during the evolution from dinuclear to mononuclear regimes.

this schematic model should be only approximately valid. We have shown that the frozen assumption [11] is satisfied. This means that during the evolution process from dinuclear to mononuclear regimes the neck length of the system is close to zero. Therefore, as far as the early dynamics of the neck growth is concerned, the approximate approach of the neck shape may not be critical. In this sense, the results obtained in this work should be acceptable. Another approximation in the present approach of the neck dynamics is that the shell structure of the colliding nuclei is not taken into account. The shell energy will resist neck growth. However, as shown in Fig. 3, the center of the radial momentum distribution is close to zero, indicating an almost complete damping of the incident energy resulting from friction between the colliding nuclei. Correspondingly, the system at contact is already heated up, and the shell structure most probably has been washed out.

## VI. SUMMARY

We have reevaluated the  $^{136}\text{Xe}(^{136}\text{Xe}, xn)^{272-x}\text{Hs}$  reaction with a modified fusion-by-diffusion model proposed here. The capture probability has been calculated using the surface friction model and the dynamic evolution from dinuclear to mononuclear regimes is taken into account by means of the two-dimensional Langevin equation. Our results show that

transition from dinuclear to mononuclear regimes takes place in a very short time, about a few times  $10^{-22}$  s. In addition, we have the distribution of the separation  $s$  between the surfaces of two approaching nuclei at the injection point in the asymmetric fission valley. In this way,  $s$  is no longer an adjustable parameter. More importantly, the quasifission competition in the early period of neck motion has been included in the present calculation. The results show that in the  $^{136}\text{Xe} + ^{136}\text{Xe}$  reaction more than 80% of the quasifission events occur during the transition from dinuclear to mononuclear regimes. Owing to the quasifission competition at the early stages of collective motion the formation cross section of hassium isotopes ( $Z = 108$ ) in the  $^{136}\text{Xe} + ^{136}\text{Xe}$  reaction is greatly reduced. Our calculated maximum values of the evaporation residue cross section in  $1n$  and  $2n$  channels are on the order of 0.5 pb, which is well below the present experimental limit for registering the evaporation residual nuclei. Thus we have clearly demonstrated the essential importance of the early dynamics of neck growth in the formation of superheavy nuclei.

## ACKNOWLEDGMENTS

This work was supported by the National Natural Science Foundation of China under Grant Nos. 10735100 and 10875013.

- 
- [1] Yu. Ts. Oganessian *et al.*, *Phys. Rev. Lett.* **83**, 3154 (1999); *Nature (London)* **400**, 242 (1999).
  - [2] Yu. Ts. Oganessian *et al.*, *Phys. Rev. C* **69**, 054607 (2004).
  - [3] Yu. Ts. Oganessian *et al.*, *Phys. Rev. C* **70**, 064609 (2004).
  - [4] Yu. Ts. Oganessian *et al.*, *Phys. Rev. C* **72**, 034611 (2005); **69**, 021601(R) (2004).
  - [5] Yu. Ts. Oganessian *et al.*, *Phys. Rev. C* **74**, 044602 (2006).
  - [6] V. Zagrebaev and W. Greiner, *Phys. Rev. C* **78**, 034610 (2008).
  - [7] G. Royer and B. Remaud, *Nucl. Phys. A* **444**, 477 (1985).
  - [8] Yu. Ts. Oganessian *et al.*, *Phys. Rev. C* **79**, 024608 (2009).
  - [9] K. Siwek-Wilczyńska, I. Skwira-Chalot, and J. Wilczyński, *Int. J. Mod. Phys. E* **16**, 483 (2007).
  - [10] W. J. Swiatecki, K. Siwek-Wilczyńska, and J. Wilczyński, *Acta Phys. Pol. B* **34**, 2049 (2003).
  - [11] W. J. Swiatecki, K. Siwek-Wilczyńska, and J. Wilczyński, *Phys. Rev. C* **71**, 014602 (2005).
  - [12] Y. Aritomo, *Phys. Rev. C* **80**, 064604 (2009).
  - [13] Z. H. Liu and J. D. Bao, *Phys. Rev. C* **80**, 034601 (2009).
  - [14] S. Cohen and W. J. Swiatecki, *Ann. Phys. (NY)* **22**, 406 (1963).
  - [15] Yu. Ts. Oganessian, *J. Phys. G* **34**, R165 (2007).
  - [16] D. H. E. Gross and H. Kalinowski, *Phys. Rep.* **45**, 175 (1978).
  - [17] J. Marten and P. Fröbrich, *Nucl. Phys. A* **545**, 854 (1992).
  - [18] G. Kosenko *et al.*, *J. Nucl. Radiochem. Sci.* **3**, 19 (2002).
  - [19] Y. Abe, D. Boilley, G. Kosenko, and C. W. Shen, *Acta Phys. Pol. B* **34**, 2091 (2003).
  - [20] W. J. Swiatecki, *Phys. Scr.* **24**, 113 (1981).
  - [21] C. E. Aguiar, V. C. Barbosa, and R. Donangelo, *Nucl. Phys. A* **517**, 205 (1990).
  - [22] K. Zhao, Z. X. Li, X. Z. Wu, and Z. X. Zhao, *Phys. Rev. C* **79**, 024614 (2009).
  - [23] G. G. Adamian, N. V. Antonenko, and R. V. Jolos, *Nucl. Phys. A* **584**, 205 (1995).
  - [24] L. G. Moretto and J. S. Sventek, *Phys. Lett. B* **58**, 26 (1975).
  - [25] Z. H. Liu and J. D. Bao, *Phys. Rev. C* **74**, 057602 (2006).
  - [26] Z. H. Liu and J. D. Bao, *Phys. Rev. C* **76**, 034604 (2007).
  - [27] Z. H. Liu and J. D. Bao, *Phys. Rev. C* **80**, 054608 (2009).